

A NUMERICAL STUDY OF THE EVOLUTION OF AIRBORNE DUST PARTICLE SIZES DURING A SIMULATED MARTIAN GLOBAL DUST STORM. M. A. Kahre¹, J. L. Hollingsworth¹, R. M. Haberle¹, and J. R. Murphy², ¹NASA Ames Research Center, Space Science Division, Moffett Field, CA, ²Department of Astronomy, New Mexico State University, Las Cruces, NM.

Introduction: Suspended dust plays a critical role in determining the thermal structure of the Martian atmosphere and consequently affects dynamical processes [1,2]. Radiative properties of airborne dust such as the single scattering albedo and the asymmetry parameter have been shown to depend on the size, composition, and shape of dust grains [3]. Mie theory predicts that the visible-to-infrared opacity ratio of dust depends on the effective radius and the variance of the particle size distribution that describes the dust population [3,4]. The dust particle size distribution most likely varies in space and time, which means that a full understanding of the radiative and dynamical effects of airborne dust on the Martian climate necessarily includes a complete understanding of the mechanisms by which the properties of the dust size distribution change.

It is reasonable to expect that the distribution of dust particle sizes in the Martian atmosphere changes in time and space. According to the Cunningham Stokes relationship, large particles fall through the Martian atmosphere at velocities greater than small particles. Because these varying fall speeds affect the suspension lifetimes of particles of different sizes, one would expect particle size segregation as a function of altitude. Furthermore, one might expect that vertical particle size segregation would likely lead to horizontal particle size segregation as well due to varying wind speeds at different altitudes.

Several authors have used spacecraft data to independently infer the particle size distribution of Martian airborne dust. Recent work indicates that, on average, the effective particle radius ranges between 1.5-1.7 μm [4,5,6,7]. Until the work of [7] and [4], interpretations of observations did not account for spatial or temporal evolution of atmospheric dust particle sizes [3]. However, [7] and [4] found that the effective particle size of airborne dust varies in both time and space. At the peak of the 2001 global dust storm, TES-derived particle effective radii ranged from approximately 1.0 to 2.5 μm [4,7].

The goal of this work is to increase our understanding of physical processes that give rise to the spatial and temporal variability of airborne particle sizes in the atmosphere of Mars. We show that the NASA Ames Mars General Circulation Model (MGCM) qualitatively captures the observed degree of temporal and spatial dust particle size variability, and we discuss

the importance of atmospheric transport in the evolution of atmospheric dust particle sizes during a simulated global dust storm.

Numerical Model and Simulation Setup: The numerical tool used for this study, the NASA Ames MGCM, is a global 3-D grid point model of the Martian atmosphere [8]. The version used here includes a fully interactive dust cycle, which includes the lifting, transport and gravitational sedimentation of radiatively active dust [9]. The model includes parameterizations for wind stress and dust devil surface dust lifting. Dust injected into the atmosphere by these two parameterizations for lifting is partitioned into a log-normal distribution with an effective radius of 2.5 μm . Dust is transported in the atmosphere horizontally and vertically by model-resolved winds. Net vertical transport is dictated by the model's vertical winds, turbulent mechanical mixing, and size-dependent gravitational settling.

The simulation presented here includes the interactive dust cycle described above with ten particle sizes ranging from 0.1 to 10 μm in radius. The wind stress and dust devil lifting parameterizations have been tuned to generate both a background dust opacity during northern summer that is consistent with observations [10] and a global dust storm during northern winter. This simulation was initiated with a planetwide infinite surface dust reservoir. When the local surface conditions enable dust lifting by either of the two dust lifting parameterizations, the appropriate amount of dust is injected into the bottom layer of the atmosphere if there is no surface CO_2 ice present. The simulation was run for one year to equilibrate the CO_2 cycle before any analyses were performed. The results presented here are from the second year of simulation.

Comparisons with Observations of Dust Particle Size Variability: We must first develop confidence in the model's ability to reproduce the observed degree of spatial and temporal variability of dust particle sizes. [7] and [4] find substantial spatial and temporal variability in derived atmospheric dust particle sizes from TES emission phase functions (EPFs) and TES spectral data during the year of the 2001 global dust storm. The authors make the assumption that the distribution of particles sizes remains constant with height. As they note and as will be shown in this work, this as-

sumption is an oversimplification due to the varying fall speeds for particles of different sizes. For this reason, we aim to make qualitative, not quantitative, comparisons between the TES-derived and model simulated spatial and temporal variability of atmospheric particle sizes.

In order to compare with the TES-derived results, we calculate effective radii based on simulated dust particle distributions. In order to assign an effective radius and variance to each column of dust, a set of idealized distributions is computed based on a matrix of effective radii and variances. The χ^2 is then minimized between the simulated particle distribution and the idealized distribution. Consistent with the variances derived from TES data, resulting variances from these fits are consistently near 0.4 [7]. The resulting best-fit column integrated effective dust particle sizes are then analyzed for both temporal and spatial variability in order to compare to TES-derived dust particle size temporal and spatial variability.

Comparisons between the TES-derived and simulated temporal variability at four specific locations (three chosen by [7] and one additional location that showed substantial simulated temporal variation in dust particle effective radius) suggest that the model qualitatively captures the observed degree of particle size variability (Fig. 1; top). Simulated column integrated effective dust particle sizes range from approximately 1.25 to 2.5 μm in radius over the course of one annual cycle. This range of values is generally consistent compared to the TES-derived results.

[7] chose to present TES-derived spatial results of effective dust particle sizes near the peak of the 2001 global dust storm ($L_s=213$). To make the most direct comparison to their results, we have chosen to examine the simulated spatial variability of effective particle sizes near the peak of the simulated global dust storm ($L_s=270$). The simulated degree of spatial variability in particle effective radius qualitatively agrees with the TES-derived particle sizes (Fig. 1; bottom). In the four longitude corridors, both simulated and TES-derived effective particle radius values exhibit a latitudinal gradient. The maximum simulated effective radius at this season in these longitude corridors is approximately 2.5 μm , which is only slightly low compared to the maximum effective radius values derived from TES data. The general spatial variability of the observations appears to be well-captured by the model.

The model qualitatively reproduces the temporal and spatial variability in atmospheric dust particles sizes. Therefore, we have confidence in utilizing the model to investigate the manner in which the spatial

pattern of airborne dust particle sizes changes over the course of a simulated global dust storm.

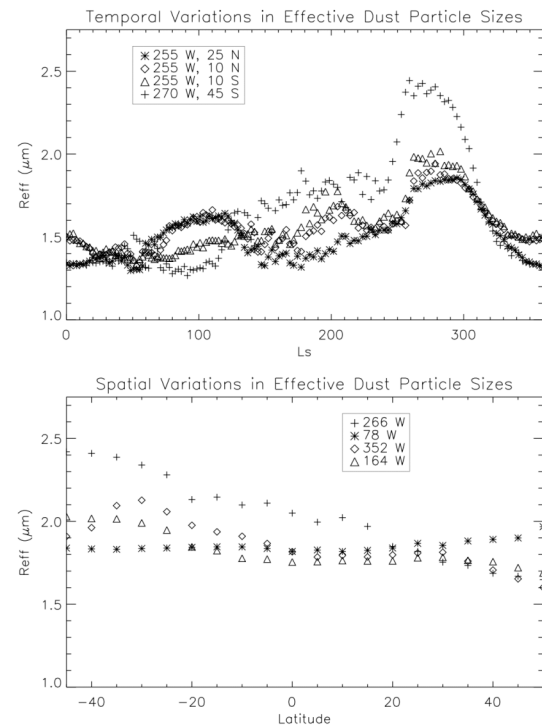


Fig 1: Top: Simulated temporal variability in column-integrated atmospheric dust particle sizes at four locations. Bottom: Simulated spatial variability in column-integrated atmospheric dust particles sizes in four longitude corridors at $L_s = 270$.

Airborne Dust Particle Size Evolution During a Simulated Global Dust Storm: While our primary interest here is related to the spatial and temporal evolution of atmospheric dust particle sizes during a global dust storm, it is important to first establish the general character of the simulated dust storm within which this evolution takes place. Simulated dust lifting begins in the Hellas region at approximately $L_s = 240$, due to increased surface wind stress on the northeast and southwest flanks of Hellas. The storm (as represented by the globally averaged dust opacity) peaks at about $L_s = 270$, at which time the globally averaged atmospheric visible dust opacity exceeds 2. The simulated global dust storm subsides when the dust source in Hellas disappears. The globally averaged visible dust opacity drops below unity at approximately $L_s = 330$.

Within the simulated global dust storm, the vertical and meridional spatial patterns of atmospheric dust particle sizes change over time. In particular, there is significant vertical variation in dust particle sizes, as one would expect given the varying fall lifetimes of

particles of different sizes. After the initiation of the simulated global dust storm, an enhancement of increased dust particle sizes extends vertically in the southern hemisphere and northward aloft (Fig. 2). This simulated dust particle size enhancement is due to an elevated dust shelf of particles ranging from 0.5 to 2.2 μm in radius that develops centered at approximately the 1 mb pressure level. This dust shelf results from dust lifting in the southern hemisphere, upward dust transport over southern middle latitudes and northward dust transport aloft through the southern middle latitudes to northern middle latitudes. The magnitude of northward dust transport between the 1 mb and 0.1 mb pressure levels for dust particles between 0.5 and 2.2 μm in radius is more than 10 times greater than the downward dust transport of these particles over middle northern latitudes. Because of this difference between horizontal and vertical transport in this altitude range, medium-sized particles build-up and create the enhancement of increased effective dust particle radii aloft. As time progresses, the source of dust from the southern hemisphere decreases (resulting in the dissipation of the storm) and the enhancement of dust particles aloft in the north decreases. This allows the enhancement in effective dust particle sizes to relax back to nearly a pre-dust storm state.

Summary: The NASA Ames Mars General Circulation Model is utilized with interactive dust lifting and radiatively active dust transport and sedimentation to investigate the transport processes that give rise to spatial and temporal variability of airborne dust particle sizes. The model-generated degree of spatial and temporal size variability is qualitatively consistent with that derived from TES data. As expected, there is significant vertical variation in dust particle sizes throughout the simulation. Additionally, we discuss in detail the manner in which the spatial pattern of airborne dust particles evolves during a simulated global dust storm.

References: [1] Gierasch P. J. and Goody R. M. (1968) *Plan. Space Sci.*, 16, 615. [2] Haberle R. M. et al. (1982) *Icarus*, 50, 322. [3] Toon O. B. et al. (1977) *Icarus* 30, 663–696. [4] Clancy R. T. et al. (2003) *JGR* 108, E9. [5] Pollack J. B. et al. (1995) *JGR* 100, 5235. [6] Tomasko M. G. et al. (1999) *JGR* 104, 8987. [7] Wolff M. J. and Clancy R. T. (2003) *JGR* 108, E9. [8] Haberle R. M. et al. (1999) *JGR* 104, 8957. [9] Kahre M. A. et al. (2006) *JGR* 111, 6008. [10] Smith, M. D. (2004) *Icarus* 167, 148-165

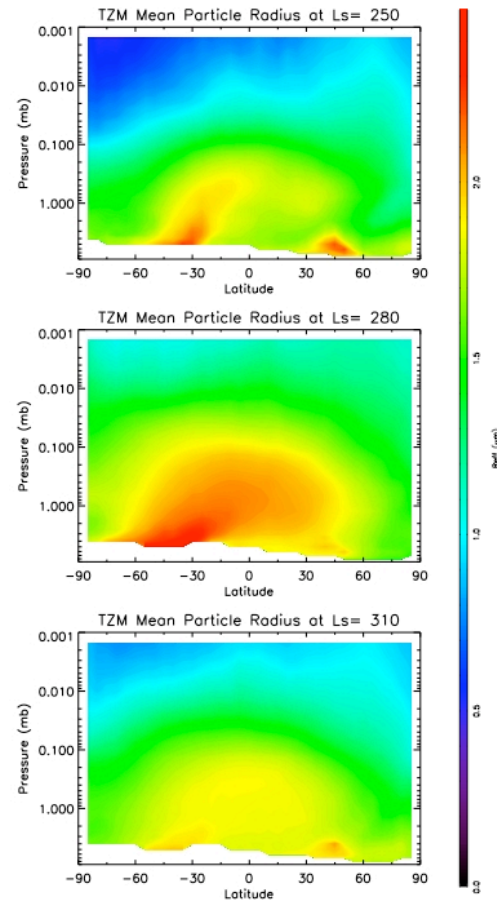


Fig 2: Time and zonal mean atmospheric effective dust particle radii at Ls = 250, 280, and 310. The peak of the simulated global dust storm occurred at approximately Ls = 270.